

Synchronization and stochastic resonance of the small-world neural network based on the CPG

Qiang Lu · Juan Tian

Received: 20 July 2013 / Revised: 19 October 2013 / Accepted: 7 November 2013 / Published online: 13 November 2013
© Springer Science+Business Media Dordrecht 2013

Abstract According to biological knowledge, the central nervous system controls the central pattern generator (CPG) to drive the locomotion. The brain is a complex system consisting of different functions and different interconnections. The topological properties of the brain display features of small-world network. The synchronization and stochastic resonance have important roles in neural information transmission and processing. In order to study the synchronization and stochastic resonance of the brain based on the CPG, we establish the model which shows the relationship between the small-world neural network (SWNN) and the CPG. We analyze the synchronization of the SWNN when the amplitude and frequency of the CPG are changed and the effects on the CPG when the SWNN's parameters are changed. And we also study the stochastic resonance on the SWNN. The main findings include: (1) When the CPG is added into the SWNN, there exists parameters space of the CPG and the SWNN, which can make the synchronization of the SWNN optimum. (2) There exists an optimal noise level at which the resonance factor Q gets its peak value. And the correlation between the pacemaker frequency and the dynamical response of the network is resonantly dependent on the noise intensity. The results could have important implications for biological processes which are about interaction between the neural network and the CPG.

Keywords Small-world neural network · CPG · Synchronization · Stochastic resonance

Introduction

The neurons have the ability of receiving environmental stimuli, information transmission and processing. Neurons can demonstrate various types of activity; tonically spiking, bursting as well as silent neurons are frequently observed in electrophysiological experiments (Rabinovich et al. 2006). Through these different spiking modes, the nervous system can deliver and process the biological neural information.

Many models have explained the spiking activities, especially the Rulkov's model (Rulkov 2002). Rulkov et al. (2004) established the model that replicates the dynamics of spiking and spiking-bursting activity of real biological neurons. Rulkov (2001) also modeled the individual dynamics of each cell with a simple two-dimensional map that produces chaotic bursting behavior similar to biological neurons. Therefore, the Rulkov's two-dimensional neural map model can be used to simulate the brain neuron. Through evidence from biological experiments, the researchers have found the brain has many features of a small-world network (Reijneveld et al. 2007; Liao et al. 2011; Li and Li 2011; van den Heuvel et al. 2008). The small world structure of neural networks reflects an optimal configuration associated with rapid synchronization and information transfer, minimal wiring costs, resilience to certain types of damage, as well as a balance between local processing and global integration (Hong et al. 2002). The synchronization and the stochastic resonance are two important characters in the brain (Wang and Wong 2013; Gao and Wang 2012). Wang et al. (2013) studied the properties of equilibria and phase synchronization involving burst synchronization and spike synchronization of two electrically coupled HR neurons. Yu et al. (2012a) investigated the stochastic resonance in the SWNN.

Q. Lu (✉) · J. Tian
College of Information and Engineering, Taishan Medical
University, Taian 271016, China
e-mail: luqiang271016@163.com

Since Matsuoka (1985, 1987) established the CPG model, the CPG has been widely applied to robot control, modeling and motion simulation of human and made great progress (Liu et al. 2011; Wu and Ma 2010) because the CPG has a salient property that it generates rhythmic movements. It is well known that the central nervous system plays a key role in humans' locomotion. The accurate movement, such as walking gait, requires cognitive processes, which are controlled by neural circuits involving the system (Takakusaki and Okumura 2008). The basic mechanisms of locomotion control are located in the spinal cord, and the spinal cord is composed of the CPG, pattern formation and motor output (Drew et al. 2004).

Many researchers have studied the relationship between the neural network and the locomotion. Harris-Warrick (2011) thought that neuromodulators determine the active neuronal composition in the CPG and it is not possible to model the function of neural networks without including the actions of neuromodulators. Maria (2010) proposed that locomotion requires a plethora of sensorimotor interactions that occur throughout the nervous system, and sensory feedback plays a crucial role in the rhythmical muscle activation pattern. However, few researchers explained the effects on the brain based on the CPG. In this paper, we focus on the synchronization and stochastic resonance of the SWNN based on the CPG and hope our findings have important implications for weak CPG signal detection and information propagation across neural networks.

This paper is organized as follows. In Section “Model between the SWNN and the CPG”, a new model showing the interaction between the SWNN and the CPG is presented according to biological knowledge and numerical simulation. Detailed analysis for the synchronization and the stochastic resonance of the SWNN based on the CPG is shown in Section “Analysis on synchronization and stochastic resonance”. The conclusions and future works are made in the last section.

Model between the SWNN and the CPG

In this paper, a two-dimensional map (Rulkov 2001) is used to simulate the dynamics of individual neuron in the SWNN. The temporal evolution of each unit is described by.

$$\begin{cases} x_{i,n+1} = \frac{\alpha_i}{1 + x_{i,n}^2} + y_{i,n} + I_{i,n}^{syn}(x_{i,n}) \\ y_{i,n+1} = y_{i,n} - \gamma x_{i,n} - \beta \end{cases} \quad (1)$$

where x_n is the fast dynamical variable representing the transmembrane voltage of the neuron and y_n is the slow dynamical variable denoting the slow gating process. The

first variable can emulate the spiking-bursting activity of a neuron, depending on the value of the parameter α , whereas the latter variable undergoes a slow temporal evolution due to the small value of the parameters β and γ , which model the action of an external dc bias current or the synaptic inputs to the cell. $I_{i,n}^{syn}(x_{i,n})$ is the coupling term, the form of which depends on the network topology chosen to describe the neural network. For a commonly investigated model of the neural network, global coupling network, the coupling term usually considers the mean field produced by all the neurons.

$$I_{i,n}^{syn}(x_{i,n}) = \frac{\varepsilon}{k_i} \sum_{j=1}^M x_{j,n}$$

where M is the number of neurons in the ensemble, and we assume that each unit i is connected with a set M comprising k_i ; other units are randomly chosen along the network. The parameter ε is the coupling strength.

According to Eq. 1, the different states of the chaotic neural map can be obtained by modulating the parameter α when β and γ are set as 0.001, as shown in Fig. 1.

The algorithm of Watts and Strogatz (1998) is used to design the small-world network: starting with a network on a ring, in which each network node is connected to its k nearest neighbors on each side of the ring and connections (edges) are selected at random with the probability p . By increasing the probability p the architecture of the network is tuned between two extremes, regular ($p = 0$) and random ($p = 1$) networks. Small-world networks are characterized by intermediate value of the probability $0 < p < 1$. These networks have a small value of characteristic path length L , comparable with that of a random network, while get a large value of clustering coefficient C , just like a regular network. The shortest path length is defined as the average number of edges in the shortest path between any two vertices, and the clustering coefficient is the fraction of edges between the neighbors with respect to maximum possible.

In the following we consider a small-world network containing $N = 200$ map-based neurons, which is obtained from a regular ring with different values of rewiring probability p and $k = 6$ (Yu 2012b). In view of the diversity of neurons in the real biological system, we set $\alpha = 4.2$ and $\beta = \gamma = 0.001$, so that each uncoupled neuron produces chaotic bursts.

In order to quantitatively characterize the synchronization of the SWNN, we calculate the synchronization coefficient δ (Yu 2012b), which is described as:

$$\begin{cases} \delta(n) = \frac{1}{N} \sum_{i=1}^N [x_i(n)]^2 - \left[\frac{1}{N} \sum_{i=1}^N x_i(n) \right]^2 \\ \delta = \sqrt{\frac{1}{T} \sum_{n=1}^T \delta(n)} \end{cases} \quad (2)$$

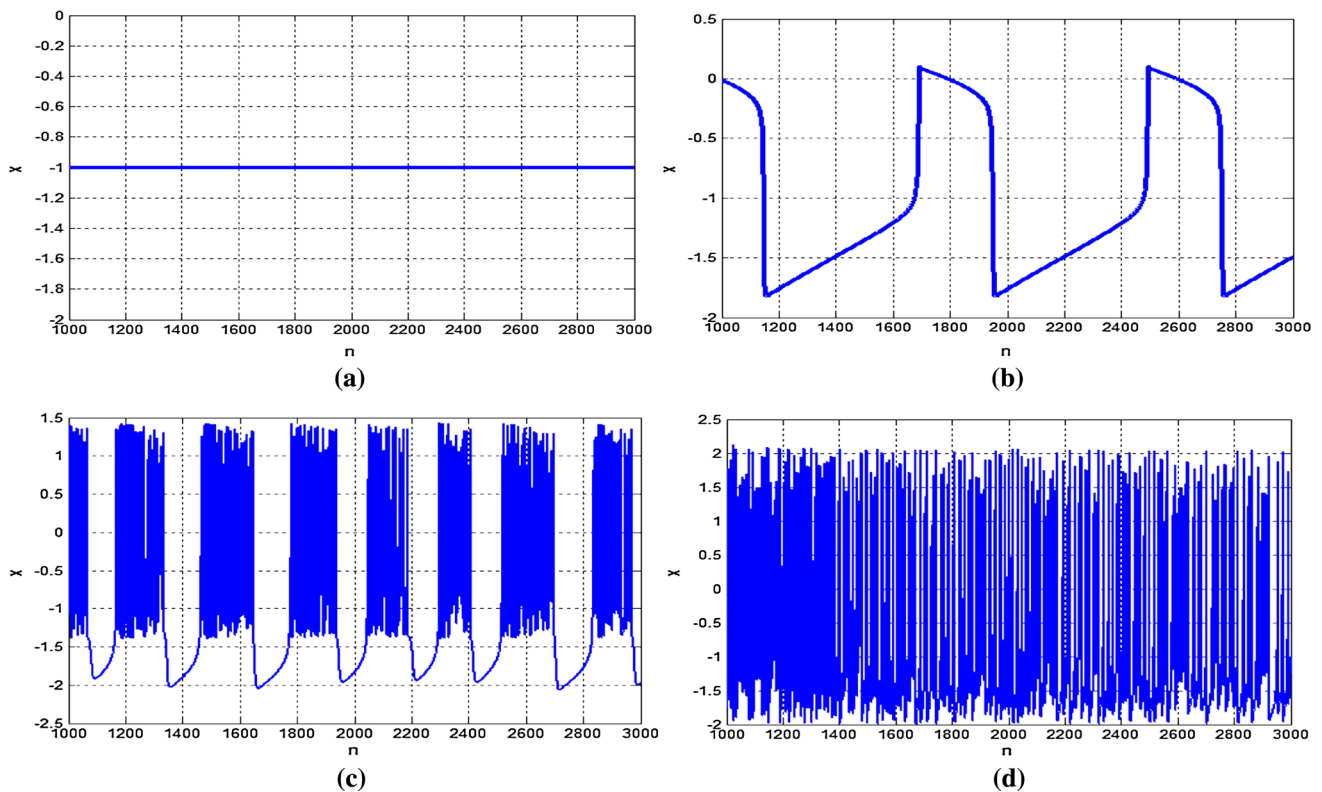


Fig. 1 Different states of the chaotic neural map. **a** Silence and $\alpha = 2$. **b** Spikes and $\alpha = 2.2$. **c** Bursts of spikes and $\alpha = 4.2$. **d** Tonic spikes and $\alpha = 5$

where T is the simulation time. The synchronization coefficient δ can describe the spatiotemporal synchronization of the neuronal firing effectively. The synchronization becomes stronger when the value of the parameter δ is close to zero. When $\delta = 0$, the state of all neurons is complete synchronization.

Another useful diagnostic of synchronization is the mean field of the ensemble and it is defined as (Yu et al. 2011).

$$X_n = \frac{1}{N} \sum_{j=1}^N x_{j,n}$$

The state of synchronized bursting in the SWNN is characterized by the large amplitude oscillation of a macroscopic mean field, whereas small amplitude fluctuations mark the absence of synchronization. A quantitative measure of synchronization is the variance of mean field oscillation $\text{Var}(X)$. The synchronization becomes stronger when the value of the variable $\text{Var}(X)$ is close to 1. When $\text{Var}(X) = 1$, the state of all neurons is complete synchronization.

According to above SWNN model, we calculate the synchronization coefficient and $\text{Var}(X)$, and the plots are exhibited in Fig. 2. In Fig. 2, the rewiring probability p is varied in the interval $[0, 1]$ in step of 0.1 and coupling

strength coefficient ε is in the interval $[0.01, 0.1]$ in step of 0.01.

From Fig. 2a, we can see that there exists an optimum interval where the synchronization is the best. In Fig. 2a, the optimum interval of the coupling strength coefficient ε is $[0.07, 0.08]$, and the rewiring probability p is $[0.2, 1]$. In Fig. 2b, with the increasing of the strength coefficient ε , the synchronization of the SWNN becomes stronger. However, when $\varepsilon > 0.08$, the value of the $\text{Var}(X)$ is smaller than $\varepsilon = 0.08$ and becomes stable. This result is in accordance with the result in Fig. 2a. In the following, we use synchronization coefficient to show the synchronization of the SWNN.

In order to confirm the number of network nodes which are connected with the CPG, we consider eleven patterns which include one node, 10, ..., 100 nodes and the step is 10. The rewiring probability p is set as 0.6 and the coupling coefficient ε is in the interval $[0.01, 0.1]$ in step of 0.01. Then the diagram of the synchronization coefficient is shown in Fig. 3.

From Fig. 3, we can see that the synchronization coefficient is becoming bigger with the increase of the number of the nodes. In other words, the synchronization is optimum when the number of nodes is one. This result is in accordance with physiological phenomenon (Gao and Wang 2011). In central nervous system, when signal is

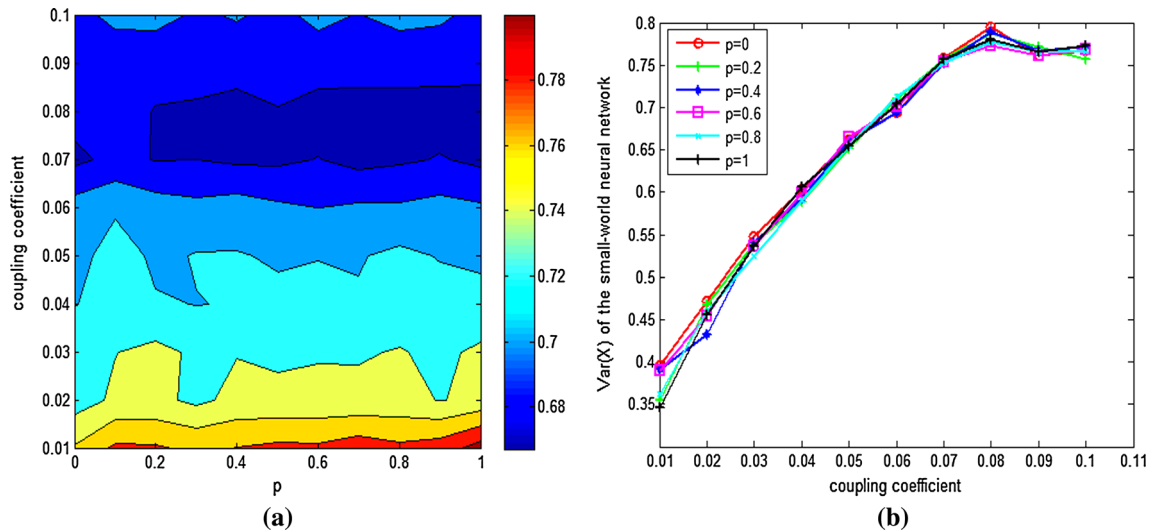
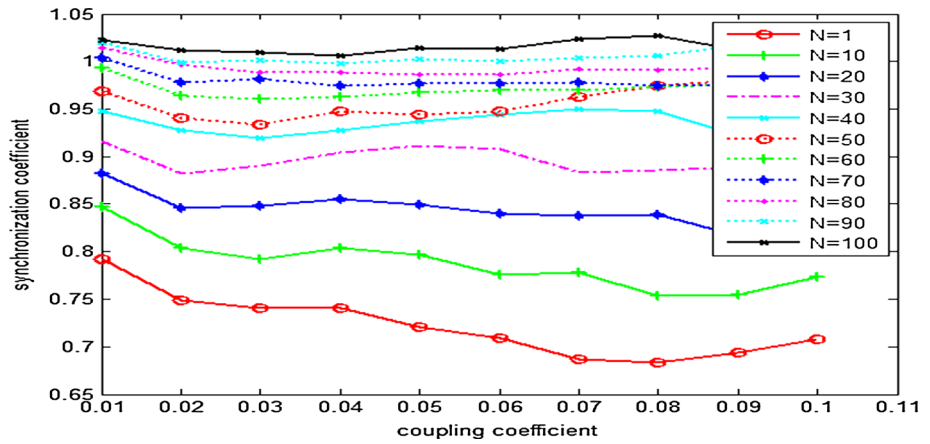


Fig. 2 Contour plot of the synchronization coefficient δ and $\text{Var}(X)$ in the SWNN. **a** Contour plot of the synchronization coefficient δ . **b** $\text{Var}(X)$

Fig. 3 The diagram of the synchronization coefficient with different number of nodes



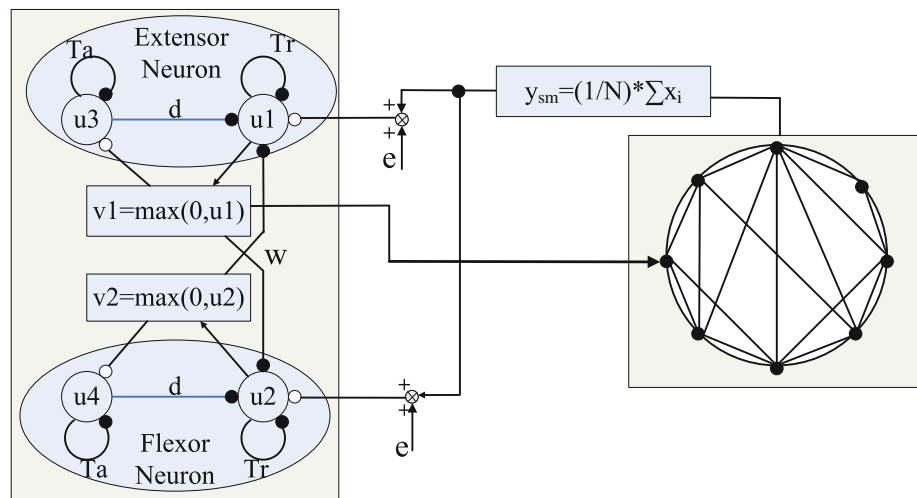
imposed on one neuron, spikes are accordingly generated in the neuron and transmitted to other neurons by means of synaptic coupling. Most neurons communicate with each other by the means of spike trains, which is believed to support information processing in the brain.

According to physiological principle, the signals from the central nervous system are transmitted to the CPG, and information from the CPG is transmitted to the central nervous system via ascending tract neurons (Takakusaki and Okumura 2008). Then we apply the periodic signal of the CPG to one arbitrarily neuron who has maximal number of neighbors (Wang et al. 2006). Stam et al. (2010) and Ponten et al. (2010) used a network of 32 connected neural masses to demonstrate how an interaction between dynamics and connectivity can explain the emergence of complex network features. This network model considers the average activity in relatively large groups of interacting

excitatory and inhibitory neurons. They all showed that the average properties like mean voltage and firing rates are efficient to understand the signals and structural connectivity of the brain. Therefore, the SWNN is taken as a whole and the mean value of all neurons is added to the input of the CPG. Then the new model between the SWNN and the CPG is shown by.

In Fig. 4, the variable y_{sm} denotes the mean value of all neurons, and the left part is CPG model (Matsuoka 2011; Zhang 2004) which includes the extensor neuron and the flexor neuron. The two variables u_1 and u_3 (u_2 and u_4) are coupled together in such a way that the output of one variable suppresses the other variable, and vice versa. Together with other parameters, the reciprocal inhibition works to produce a stable oscillation. The output of one neuron is added to the other neuron and the output of the CPG is v_j . The model of the CPG can be described by.

Fig. 4 The model between the SWNN and the CPG



$$\begin{cases} T_r \dot{u}_1 + u_1 = -du_3 - wg(u_2) + e \\ T_r \dot{u}_2 + u_2 = -du_4 - wg(u_1) + e \\ T_a \dot{u}_3 + u_3 = g(u_1) \\ T_a \dot{u}_4 + u_4 = g(u_2) \\ v_1 = g(u_1) \end{cases} \quad (3)$$

The function $g(\cdot)$ is a piecewise linear function defined by $g(u) = \max(0, u)$, which represents a threshold property of the neurons. These variables u_1, u_3 and v_1 represent the membrane potential and the firing rate of the neuron, respectively. Self-inhibitory input u_2 and u_4 represent an adaptation or fatigue property that ubiquitously exists in real neurons. The parameter e denotes the tonic input. Parameters w and d represent the strength of mutual and self inhibition, respectively; parameters T_r and T_a are the time constants that determine the reaction times of variables u_1, u_3 and u_2, u_4 . In the following these parameters are set as $T_r = 0.1, T_a = 2T_r, w = d=2.5$ and $e = 2$ (Matsuoka 2011).

Analysis on synchronization and stochastic resonance

The synchronization on the SWNN based on the CPG

The frequency of the CPG is proportional to $1/T_r$ or $1/T_a$ and the amplitude of the CPG is proportional to the parameter e (Matsuoka 2011). In this paper, we modulate the values of the parameter T_r and e to change the frequency and amplitude of the CPG. In order to investigate the effects on the SWNN when the frequency of the CPG is varied, the parameter T_r is in the interval $[0.1, 0.19]$ in step of 0.01. The rewiring probability p is varied in the interval $[0, 1]$ in step of 0.1 and the coupling strength coefficient ε is in the interval $[0.01, 0.1]$ in step of 0.01. Then the

diagram of the synchronization coefficient is obtained in Fig. 5. Figure 5a–d correspond to $p = 0.1, 0.5, 0.7, 1$, respectively. However, $T_r = 0.15$ and the parameter p is varied in Fig. 5e.

Comparing with no signal input, the synchronization of the SWNN is changed because of the CPG input. When $T_r = 0.15$ and $\varepsilon = 0.08$, the synchronization is optimum in Fig. 5a–d. From Fig. 5e, we also can see that there exists an optimum rewiring probability whose value is 0.5 or 1.

Now we investigate effects on the SWNN when the amplitude of the CPG is varied. The parameter e is in the interval $[1, 10]$ in step of 1 and $T_r = 0.15$. Then the diagram of the synchronization coefficient is obtained in Fig. 6. Comparing with no signal input, the synchronization of the SWNN is changed because the amplitude of the CPG is varied. With the increase of the parameter e , the synchronization of the SWNN becomes weaker. There exists optimum parameters space where $p = 1, e = 1$ and $\varepsilon = 0.08$.

When no signal is added to the SWNN, in other words, no perturbation, therefore, the synchronization of the SWNN is better. However, neurons, an important class of excitable systems, are constitutive elements of the biological brain (Gao and Wang 2011). The signal above a small threshold can make the nervous system undergo large excursions before eventually returning to the original rest state. From Figs. 5 and 6, we can see this phenomenon. In Figs. 5e and 6e, it is obvious that increasing the parameter p lead to an enhancement of synchronization of the SWNN when coupling coefficient is 0.08 (Ozer et al. 2009). From Figs. 5a–d and 6a–d, we can see the changes of two parameters T_r and e lead to the change of the CPG signal and it affects the synchronization of the SWNN. It demonstrates that the change of the signal has effect on the dynamical behaviors of neuronal systems (Gao and Wang 2011).

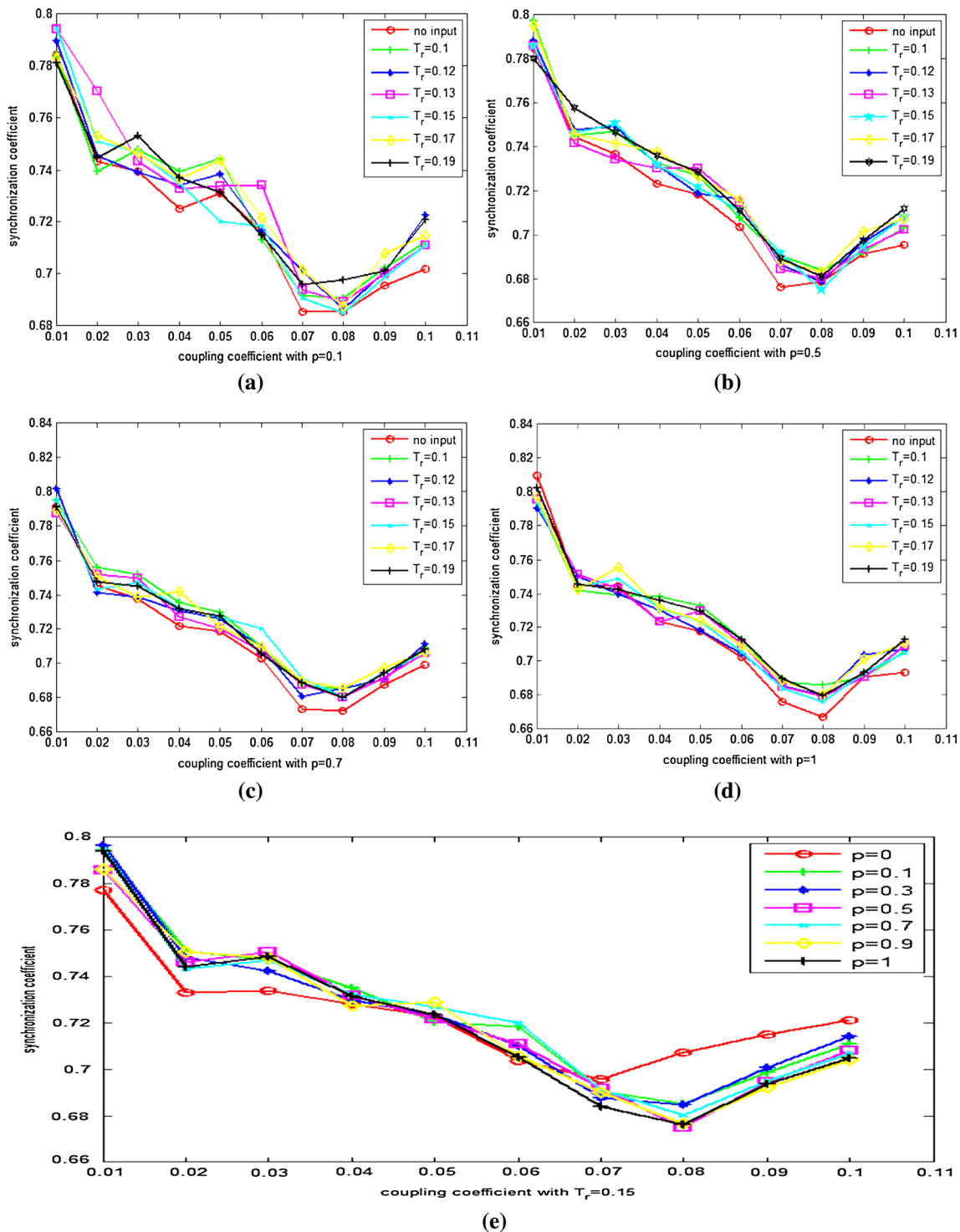


Fig. 5 Synchronization coefficient with different value of p and T_r . **a** $p = 0.1$. **b** $p = 0.5$. **c** $p = 0.7$. **d** $p = 1$. **e** $T_r = 0.15$

The effects on the CPG with the SWNN feedback

The SWNN is taken as a whole and the mean value of all neurons is added to the input of the CPG. Therefore, the feedback of the SWNN can be treated as the change of the parameter e which affects the amplitude of the CPG. The

rewiring probability p is varied in the interval $[0, 1]$ in step of 0.1 and the coupling strength coefficient ϵ is in the interval $[0.01, 0.1]$ in step of 0.01 . Then the diagram of the mean value of the SWNN is obtained in Fig. 7.

From Fig. 7a, the mean value of the SWNN is the maximum when $\epsilon = 0.04$ and $p = 1$ and the minimum is

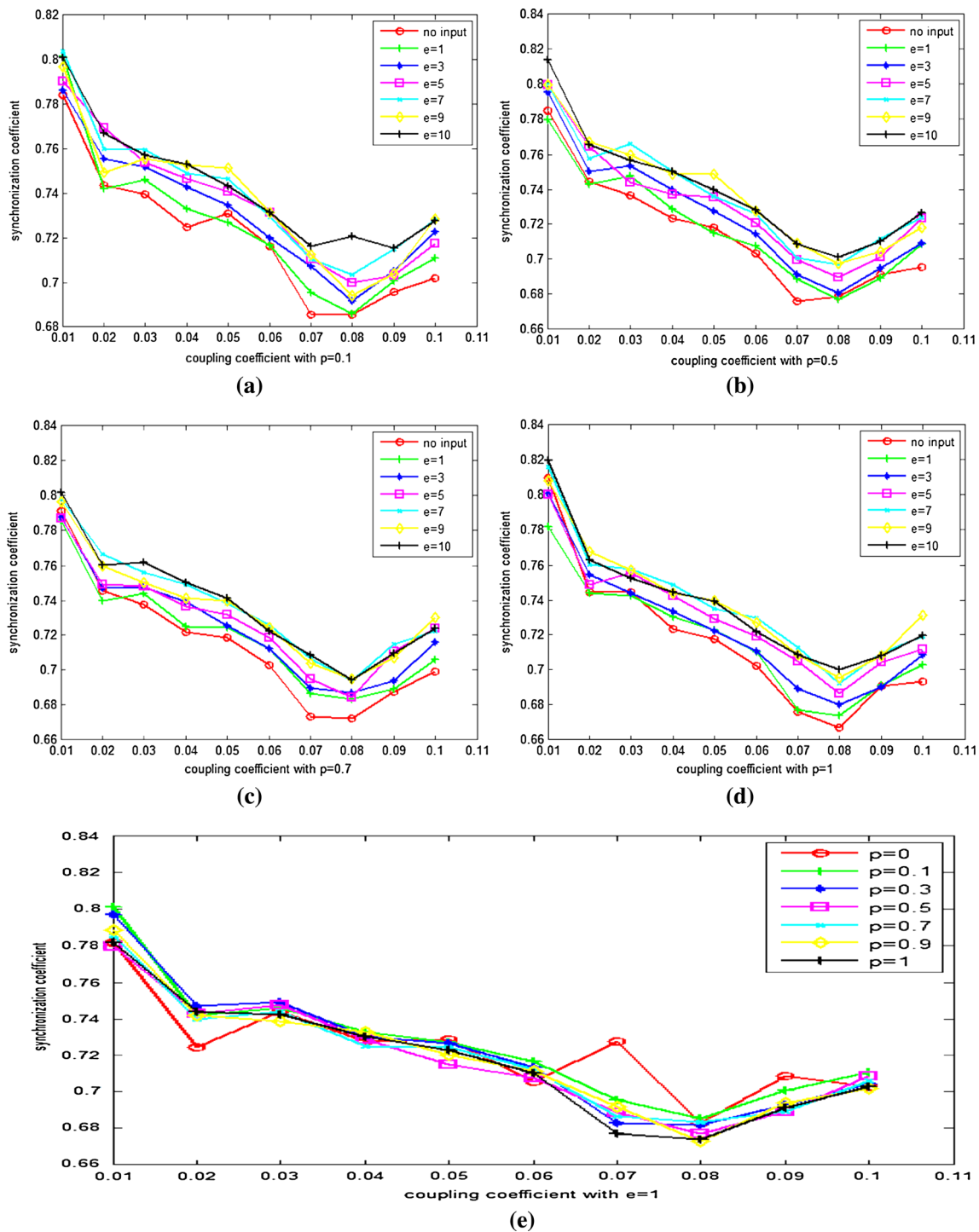


Fig. 6 Synchronization coefficient with different value of p and e . **a** $p = 0.1$. **b** $p = 0.5$. **c** $p = 0.7$. **d** $p = 1$. **e** $e = 1$

obtained when $\varepsilon = 0.08$ and $p = 1$. In Fig. 7b and Fig. 7c, the change of the SWNN output affects the amplitude of the CPG output. Then the brain can modulate the CPG and control locomotion. This result is in accordance with the result in (Takakusaki and Okumura 2008).

Stochastic resonance

The temporal evolution of each unit, along with the Gaussian noise and the coupling term, is described by (Yu 2012b).

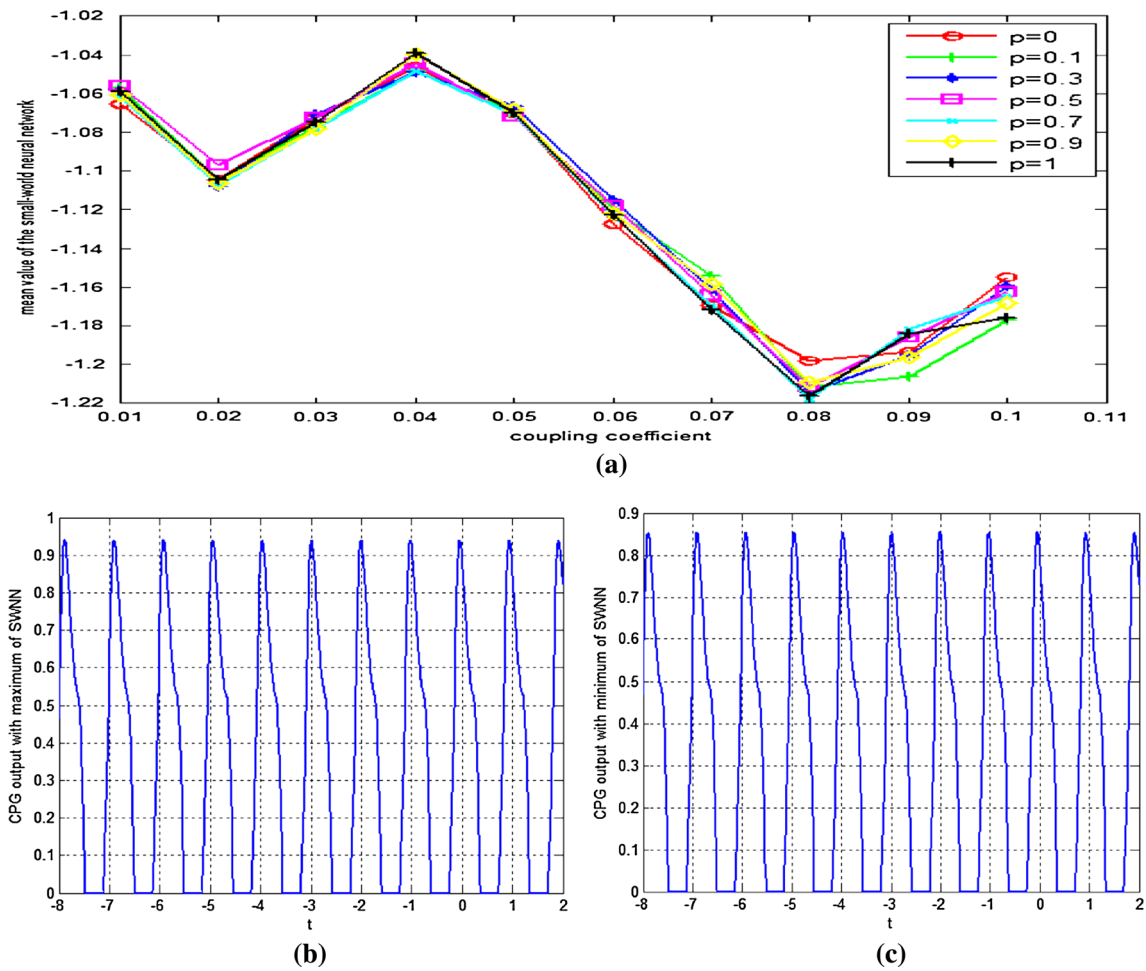
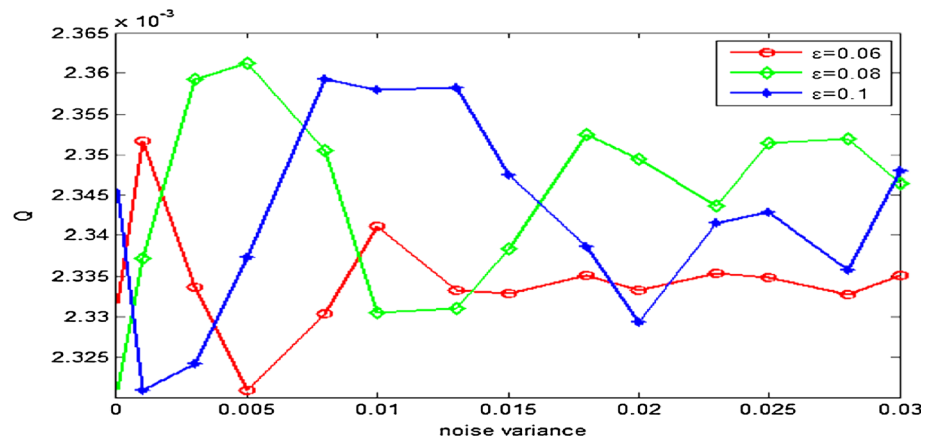


Fig. 7 Mean value of the SWNN with different value of p and CPG output. **a** Mean value of the SWNN with different value of p . **b** CPG output with maximum of SWNN. **c** CPG output with minimum of SWNN

Fig. 8 The dependence of Q on the noisy variance for different value of the parameter ε



$$\begin{cases} x_{i,n+1} = \frac{\alpha_i}{1 + x_{i,n}^2} + y_{i,n} + I_{i,n}^{syn}(x_{i,n}) + I_i^{ext}(n) + \xi_i(n) \\ y_{i,n+1} = y_{i,n} - \gamma x_{i,n} - \beta \end{cases}$$

(4)

where $I_i^{ext}(n)$ is the CPG input signal, and $\xi_i(n)$ is Gaussian noise whose mean value is zero and the variance is σ .

In order to quantitatively characterize the correlation of temporal output series of each excitable unit $x_i(n)$ with the pacemaker's frequency w , we calculate the Fourier coefficients $Q^{(i)}$ (Yu Yu 2012b), which is defined as:

$$\begin{cases} Q_{\sin}^{(i)} = \frac{1}{T} \sum_{n=1}^T 2x_i(n) \sin(\omega n) \\ Q_{\cos}^{(i)} = \frac{1}{T} \sum_{n=1}^T 2x_i(n) \cos(\omega n) \\ Q^{(i)} = \sqrt{Q_{\sin}^{(i)2} + Q_{\cos}^{(i)2}} \end{cases} \quad (5)$$

where T is the operation period of the pacemaker and $w = 1/T_r$. Since the Fourier coefficients are proportional to the square of the spectral power amplification, which is frequently used as a measure for stochastic resonance, here, we use Q as a resonance factor, which is computed as the average value of all $Q^{(i)}$ (Yu 2012b), which is described as:

$$Q = \frac{1}{N} \sum_{i=1}^N Q^i \quad (6)$$

The Gaussian noise is added in all nodes of the SWNN, and the periodic signal of the CPG is applied to one arbitrarily neuron who has maximal number of neighbors. Other parameters are set as $p = 1$, $T_r = 0.11$ and $e = 1$.

Then the dependence of Q on the noisy variance for different value of the parameter ε is plotted in Fig. 8.

It can be observed that there exists an optimal noise level at which Q gets its peak value, i.e., the temporal coherence between the temporal output series of each excitable unit and the frequency w achieves an optimum. Thus, it confirms the existence of pacemaker-driven stochastic resonance in the SWNN. Moreover, larger noise intensities are needed to evoke the optimal response with increasing ε . This result is in accordance with the result in (Yu et al. 2012a).

Conclusions

According to biological knowledge and numerical simulation, the model between the SWNN and the CPG is established. The periodic signal of the CPG is applied to one arbitrarily neuron who has maximal number of neighbors. The synchronization of the SWNN is analyzed when the amplitude and frequency of the CPG are changed and the effects on the CPG when the rewiring probability p and the coupling coefficient ε are changed. And we also study the stochastic resonance. From analysis, we can see that the synchronization of the SWNN depends on the structure of the CPG and the SWNN, such as the rewiring probability p , coupling coefficient ε , the CPG frequency parameter T_r and the amplitude parameter e . There exists an optimal noise level at which the resonance factor Q gets its peak value. And the correlation between the pacemaker frequency and the dynamical response of the network is

resonantly dependent on the noise intensity. Considering the relationship between the brain and the locomotion, the results could have important implications for many biological processes which are about the neural network. Neuroanatomic studies reveal that neurons with similar connectional and functional features are grouped into clusters which called cortical areas or subcortical nuclei (Zamora-López et al. 2011). Then the synchronization and the stochastic resonance on the modular neuronal network containing several subnetworks are deserved further investigation.

Acknowledgments The work is supported by Taian Science and Technology Development Program, China (Grant No. 20123070), and High School Science and Technology Planning of Shandong Province, China (Grant No. J13LN04).

References

- Drew T, Prentice S, Schepens B (2004) Cortical and brainstem control of locomotion. *Prog Brain Res* 143:251–261
- Gao Y, Wang J (2011) Oscillation propagation in neural networks with different topologies. *Phys Rev E* 83:031909
- Gao Y, Wang J (2012) Doubly stochastic coherence in complex neuronal networks. *Phys Rev E* 86(5):051914
- Harris-Warrick RM (2011) Neuromodulation and flexibility in Central Pattern Generator networks. *Curr Opin Neurobiol* 21(5):685–692
- Hong H, Choi MY, Kim BJ (2002) Synchronization on small-world networks. *Phys Rev E* 65:026139
- Li C, Li Y (2011) Fast and robust image segmentation by small-world neural oscillator networks. *Cognize Neurodynamics* 5:209–220
- Liao W, Ding J, Marinazzo D et al (2011) Small-world directed networks in the human brain: multivariate granger causality analysis of resting-state fMRI. *Neuroimage* 54:2683–2694
- Liu C, Chen Q, Wang D (2011) CPG-inspired workspace trajectory generation and adaptive locomotion control for quadruped robots. *IEEE Trans Syst Man Cybern B Cybern* 41(3):867–880
- Maria K (2010) Neural control of locomotion and training-induced plasticity after spinal and cerebral lesions. *Clin Neurophysiol* 121:1655–1668
- Matsuoka K (1985) Sustained oscillations generated by mutually inhibiting neurons with adaptation. *Biol Cybern* 52:367–376
- Matsuoka K (1987) Mechanisms of frequency and pattern control in the neural rhythm generators. *Biol Cybern* 56:345–353
- Matsuoka K (2011) Analysis of a neural oscillator. *Biol Cybern* 104:297–304
- Ozer M, Perc M, Uzuntarla M (2009) Stochastic resonance on Newman-Watts networks of Hodgkin-Huxley neurons with local periodic driving. *Phys Lett A* 373:964–968
- Ponten SC, Daffertshofer A, Hillebrand A et al (2010) The relationship between structural and functional connectivity: graph theoretical analysis of an EEG neural mass model. *Neuroimage* 52:985–994
- Rabinovich MI, Varona P, Selverston AI et al (2006) Dynamical principles in neuroscience. *Rev Mod Phys* 78(4):1213–1265
- Reijneveld JC, Ponten SC, Berendse HW et al (2007) The application of graph theoretical analysis to complex networks in the brain. *Clin Neurophysiol* 118(11):2317–2331
- Rulkov NF (2001) Regulation of synchronized chaotic bursts. *Phys Rev Lett* 86:183–186
- Rulkov NF (2002) Modeling of spiking–bursting neural behavior using two-dimensional map. *Phys Rev E* 65:041922

- Rulkov NF, Timofeev I, Bazhenov M (2004) Oscillations in large-scale cortical networks: map-based model. *J Comput Neurosci* 17:203–223
- Stam CJ, Hillebrand A, Wang H et al (2010) Emergence of modular structure in a large-scale brain network with interactions between dynamics and connectivity. *Frontiers in Computational Neuroscience* 4:00133
- Takakusaki K, Okumura T (2008) Neurobiological basis of controlling posture and locomotion. *Advanced Robotics* 22:1629–1663
- van den Heuvel MP, Stam CJ, Boersma M et al (2008) Small-world and scale-free organization of voxel-based resting-state functional connectivity in the human brain. *Neuroimage* 43(3):528–539
- Wang Z, Wong WK (2013) Key role of voltage-dependent properties of synaptic currents in robust network synchronization. *Neural Networks* 43:55–62
- Wang S, Xu X, Wu Z et al (2006) Effects of degree distribution in mutual synchronization of neural networks. *Phys Rev E* 74(4):041915
- Wang H, Wang Q, Lu Q et al (2013) Equilibrium analysis and phase synchronization of two coupled HR neurons with gap junction. *Cognize Neurodynamics* 7:121–131
- Watts DJ, Strogatz SH (1998) Collective dynamics of ‘small-world’ networks. *Nature* 393:440–442
- Wu X, Ma S (2010) Adaptive creeping locomotion of a CPG-controlled snaked-like robot to environment change. *Auton Robot* 28(3):283–294
- Yu H (2012) Synchronization, resonance, and control on neuronal networks. Tianjin University, Dissertation
- Yu H, Wang J, Deng B et al (2011) Chaotic phase synchronization in small-world networks of bursting neurons. *Chaos* 21:013127
- Yu H, Wang J, Liu C et al (2012) Stochastic resonance in coupled small-world neural networks. *Acta Physica Sinica* 61(6):068702
- Zamora-López G, Zhou C, Kurths J (2011) Exploring brain function from anatomical connectivity. *Frontiers in Neuroscience* 5:83
- Zhang X (2004) Biological-inspired rhythmic motion & environmental adaptability for quadruped robot. Tsinghua University, Dissertation